

# DYNAMIC APERTURE LIMITATION IN $e^+e^-$ COLLIDERS DUE TO SYNCHROTRON RADIATION IN QUADRUPOLES \*

A. Bogomyagkov <sup>†</sup>, E. Levichev, S. Sinyatkin, S. Glukhov,  
 Budker Institute of Nuclear Physics SB RAS, 630090 Novosibirsk, Russia

## Abstract

In a lepton storage ring of very high energy (e.g. in the  $e^+e^-$  Higgs factory) synchrotron radiation from quadrupoles constraints transverse dynamic aperture even in the absence of any magnetic nonlinearities. This was observed in LEP and the Future Circular  $e^+e^-$  Collider (FCC-ee). Synchrotron radiation in the quadrupoles modulates the particle energy at the double betatron frequency. Energy modulation varies transverse focusing strength at the same frequency and creates a parametric resonance of the betatron oscillations. Starting from 6d equations of motion we derive and solve the relevant differential equation describing the resonance, and show good agreement between analytical results and numerical simulation.

## INTRODUCTION

Two future electron-positron colliders FCC-ee (CERN) [1] and CEPC (IHEP, China) [2] are now under development to carry experiments in the center-of-mass energy range from 90 GeV to 350 GeV. In these projects strong synchrotron radiation (power  $\mathcal{P} \propto E^4$ ) is a source of effects negligible at low energy but essential at high energy, which influence beam dynamics and collider performance. One example is luminosity degradation caused by the particle radiation in the collective field of the opposite bunch (beamstrahlung [3]) either due to the particle loss [4] or because of the beam energy spread increase [5]. Another example is about reduction of the transverse dynamic aperture due to synchrotron radiation from quadrupole magnets. John Jowett is the first who pointed out this effect in LEP collider with maximum beam energy about 100 GeV [6]. Switching on the radiation from quadrupoles in the particle tracking decreased the stable betatron amplitude as compared to the radiation from bending magnets only. Jowett gave a description of this effect: “Here I shall briefly describe a new effect which I propose to call Radiative Beta-Synchrotron Coupling (RBSC). It is a non-resonant effect. A particle with large betatron amplitude makes an extra energy loss by radiation in quadrupoles. If you imagine that its betatron amplitude does not change much over a number of synchrotron oscillations (that is not essential to the effect), you can say that its “effective stable phase angle” will change to reflect the greater energy loss. The particle will tend to oscillate about a displaced fixed point in the synchrotron phase plane. This results in a growth of the oscillation amplitude which may eventually lead the particle outside the stable region in synchrotron

phase space.” Jowett illustrates above assertion with synchrotron phase trajectories for two stable particles (denoted by P and Q in Fig. 1) and one unstable (denoted by R) [7]. The tracking incorporates only radiation damping (quantum noise is absent) from both bending and quadrupole magnets.

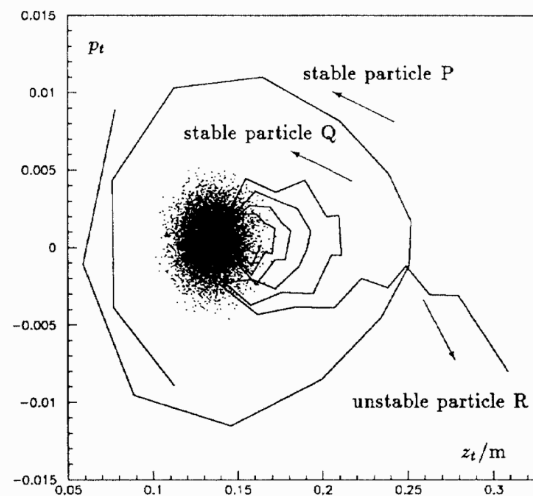


Figure 1: The vertical RBSC instability in LEP at 90 GeV projected into synchrotron phase space. Three lines show the motion of three particles P, Q and R with different initial conditions. P starts with zero betatron amplitude and large longitudinal deviation. It remains stable and damps to the equilibrium synchrotron phase. Q and R start with longitudinal coordinates corresponding to the closed orbit but with vertical amplitude 5.5 mm and 6 mm respectively. Q is stable while R’s amplitude grows in few turns until it is lost. A fourth particle has been tracked with quantum emission to give the cloud of points representing the core of the beam around the closed orbit.

In [8] Jowett has mentioned that the RBSC rarely occurs in isolation: “Most often some other effect limits the dynamic aperture before the RBSC limit is reached. In the standard (LEP) lattice the horizontal dynamic aperture is limited by a rather strong shift of the vertical tune with the horizontal action variable, bringing  $Q_y$  down onto the integer.”

Our interests to the subject was inspired by the FCC-ee lattice study. With the help of SAD accelerator design code [9] K. Oide demonstrated FCC-ee transverse dynamic aperture reduction due to radiation from quadrupoles [10], “While the radiation loss in dipoles improves the aperture, especially at  $i\bar{i}$ , due to the strong damping, the radiation loss in the quadrupoles for particles with large betatron amplitudes

\* This work has been supported by Russian Science Foundation (project N14-50-00080).

<sup>†</sup> A.V.Bogomyagkov@inp.nsk.su

reduces the dynamic aperture. This is due to the induced synchrotron motion through the radiation loss”.

We crosschecked the simulation made by Oide using MAD-X PTC [11] and the homemade software TracKing [12] including SR from quadrupoles and found good agreement between all three codes. Nevertheless, detailed consideration has shown different nature of the particle loss in horizontal and vertical planes. Radiation from quadrupoles at large horizontal amplitude indeed greatly shifts the synchronous phase, induces large synchrotron oscillation, excites strong synchro-betatron resonances and, finally, moves the horizontal tune toward the integer resonance (due to the nonlinear chromatic and geometrical aberrations) according to the mechanism described by Jowett and Oide. However, in the vertical plane the picture of the particle loss was quite different. The energy loss from radiation in quadrupoles for the vertical plane is substantially smaller than for the horizontal plane and does not provide large displacement of the synchronous phase and synchrotron oscillation. Instead, we found that increase of the vertical betatron oscillation amplitude modifies the vertical damping until, at some threshold, the damping changes to rising and the particle gets lost.

This new effect is a parametric resonance in oscillations with friction; radiation from quadrupoles modulates the particle energy at the double betatron frequency; therefore, quadrupole focusing strength also varies at the doubled betatron frequency creating the resonant condition. However, due to friction, resonance develops only if oscillation amplitude is larger than a certain value. The remarkable property of this resonance is that it occurs at any betatron tune (not exactly at half-integer) and hence can be labeled as “self-inducing parametric resonance”.

We will derive particle equations of motion in presence of the radiation from quadrupoles, consider particle loss for both transverse planes and compare results with computer simulation.

## PARAMETERS VALUES AND OBSERVATIONS FROM TRACKING

For the FCC-ee lattice “FCCee\_z\_202\_nosol\_13.seq” at 45 GeV Figs. 2 and 3 show dynamic aperture obtained by MADX PTC [11] tracking with synchrotron radiation from all magnetic elements and without. Figure 4 compares dynamic aperture with synchrotron radiation from dipoles only and dynamic aperture with radiation from dipoles and quadrupoles obtained by homemade software (TracKing [12]). The observation point is interaction point (IP).

Inclusion of synchrotron radiation in quadrupoles into tracking software decreases dynamic aperture

- in vertical direction from  $R_y = 142\sigma_y$  to  $R_y = 57\sigma_y$ ,
- in horizontal direction from  $R_x = 109\sigma_x$  to  $R_x = 65\sigma_x$ .

FCC-ee lattice has two IPs and Table 1 gives the relevant parameters.

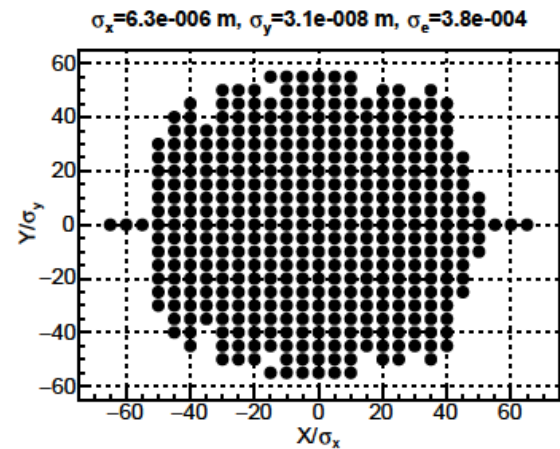


Figure 2: Dynamic aperture with synchrotron radiation from all magnetic elements, tracking by MADX PTC.

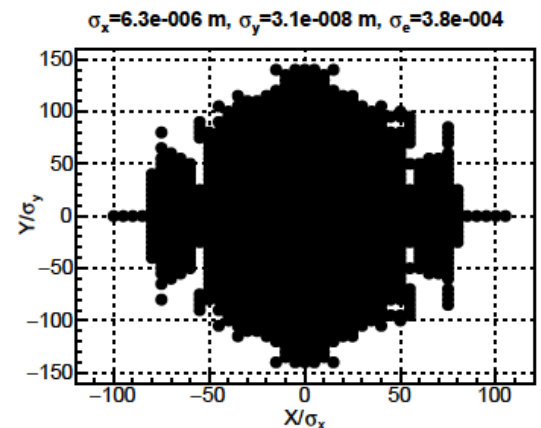


Figure 3: Dynamic aperture without synchrotron radiation from all magnetic elements, tracking by MADX PTC.

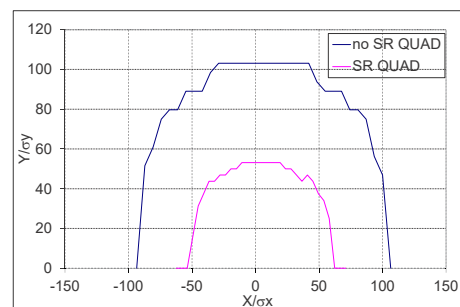


Figure 4: Dynamic aperture with synchrotron radiation from quadrupoles (blue) and without (magenta), tracking by homemade software.

Table 2 lists total synchrotron radiation energy loss from different type of magnets. For particles with vertical amplitude energy loss from final focus (FF) quadrupoles dominates the loss from the arc quadrupoles. For particles

Table 1: FCC-ee lattice parameters

$E_0$ [Gev]	45.6
tunes: $\nu_x/\nu_y/\nu_s$	269.14/267.22/0.0413
damping times: $\tau_x/\tau_y/\tau_\sigma$ [turns]	2600/2600/1300
IP: $\beta_x/\beta_y$ [m]	0.15/0.001
$\varepsilon_x/\varepsilon_y$ [m]	$2.7 \times 10^{-10}/9.6 \times 10^{-13}$
IP: $\sigma_x/\sigma_y$ [m]	$6.3 \times 10^{-6}/3.1 \times 10^{-8}$
$\sigma_\delta$	$3.8 \times 10^{-4}$

with horizontal amplitude energy losses in FF and the quadrupoles are comparable.

Table 2: Total energy loss from dipoles, final focus quadrupoles QFF, focusing and defocusing arc quadrupoles QF and QD

Type	N	$U(50\sigma_x)$ , MeV	$U(50\sigma_y)$ , MeV
Dipoles	2900	35.96	
QFF	4	12	2
QF	1470	4.1	$3.7 \times 10^{-3}$
QD	1468	1.5	$1.5 \times 10^{-2}$

Averaged over betatron phases radiation from quadrupoles is

$$U_q = \frac{C_\gamma}{2\pi} E_0^4 \oint \sum K_1^2 (x^2 + y^2) ds \quad (1)$$

$$= E_0 \Gamma \Pi [\langle K_1^2 \beta_x \rangle J_x + \langle K_1^2 \beta_y \rangle J_y],$$

where  $\Gamma = \frac{C_\gamma}{2\pi} \frac{E_0^4}{p_0 c}$  is radiation related factor,  $\Pi$  is circumference, and the corresponding lattice integrals are

$$\langle K_1^2 \beta_x \rangle = 4 \times 10^{-3} \text{ m}^{-3},$$

$$\langle K_1^2 \beta_y \rangle = 1.4 \times 10^{-1} \text{ m}^{-3}.$$

For understanding the reasons of particle loss we studied with tracking particle trajectories in vicinity of dynamic aperture border. Figure 5 shows phase and time trajectories of the first unstable particle with initial vertical coordinate  $y = 58\sigma_y$  and remaining five coordinates are zero. In the longitudinal plane  $\{PT, T\}$  synchrotron oscillations excited by additional power loss are damped to zero and suddenly something forces particle to walk away.

Figure 6 shows the change of envelope evolution for particles with initial vertical coordinate around the dynamic aperture boundary  $y = \{50; 52; 55; 57.5; 58; 58.5\} \times \sigma_y$ , horizontal coordinates are zero, longitudinal are chosen with respect to the new synchronous point.

Figures 7 and 8 show phase and time trajectories of the first unstable particle with initial vertical coordinate  $x = 67.1\sigma_x$  and remaining five zero. There is no damping and walking away in the longitudinal plane  $\{PT, T\}$  as in case of vertical initial conditions Fig. 5. On Fig. 8 notice the bottom left plot showing phase advance per turn with respect to turn number; the particle action starts to grow after phase advance per turn reaches an integer.

## EQUATIONS OF MOTION

We start from Hamiltonian

$$H(x, \sigma, y, p_x, p_\sigma, p_y; s) = 1 + p_\sigma + K_0 x + K_0^2 \frac{x^2}{2}$$

$$+ K_1 \frac{x^2 - y^2}{2} + K_2 \frac{x^3 - 3xy^2}{6}$$

$$- (1 + K_0 x) \sqrt{(1 + p_\sigma)^2 - p_x^2 - p_y^2}$$

$$+ \left( -\frac{eV_0}{p_0 c} \right) \frac{\lambda_{RF}}{2\pi} \cos \left( \phi_s + \frac{2\pi\sigma}{\lambda_{RF}} \right) \delta(s - s_0), \quad (2)$$

where  $c$  is the speed of light,  $p_0$  and  $E_0$  are the reference momentum and energy,  $e$  is the electron charge,  $B\rho = -e/p_0 c$  is the rigidity,  $K_0 = B_y(0)/B\rho$  is the reference orbit curvature,  $K_1 = (dB_y/dx)/B\rho$  is the normalized quadrupole gradient,  $K_2 = (d^2 B_y/dx^2)/B\rho$  is the normalized sextupole strength,  $p_\sigma = \Delta E/p_0 c$  is the longitudinal momentum,  $p_{x,y} = P_{x,y}/p_0$  are the normalized transverse momenta,  $V_0, \lambda_{RF}$  are the RF cavity voltage amplitude and wave length,  $s$  is the azimuth along the orbit,  $\sigma = s - ct$  is the longitudinal coordinate conjugate to the longitudinal momentum  $p_\sigma$ ,  $s_0$  is the position of point like RF cavity,  $\phi_s$  is the phase of RF field.

Radiation power with assumption of negligible electron mass ( $\beta = v/c = 1, E = pc$ ) is

$$\mathcal{P} = c \frac{C_\gamma}{2\pi} e^2 E^2 B^2$$

$$= c \frac{C_\gamma}{2\pi} E_0^4 \left( 1 + 2p_\sigma \right) (K_0^2 + 2K_0 K_1 x + K_1^2 (x^2 + y^2))$$

$$= c \frac{C_\gamma}{2\pi} E_0^4 \left( K_0^2 (1 + 2p_\sigma) + 2K_0 K_1 x + K_1^2 (x^2 + y^2) \right), \quad (3)$$

where  $B^2 = (B_y + x dB_y/dx)^2 + y^2 (dB_y/dx)^2$  and we dropped terms with  $p_\sigma^2$  and  $4K_0 K_1 x p_\sigma, 2K_1^2 p_\sigma (x^2 + y^2)$ .

The next step is to expand Hamiltonian Eq. (2) up to third order in all variables, neglect the term  $K_0 x (p_x^2 + p_y^2)/2$  due to its smallness, and obtain equations of motion where radiation is included by hand with the term describing the change of momenta,

$$x' = p_x - p_x p_\sigma \quad (4)$$

$$p_x' = K_0 p_\sigma - x(K_0^2 + K_1) - K_2 \frac{x^2 - y^2}{2}$$

$$- \Gamma p_x \left[ K_0^2 (1 + 2p_\sigma) + x(2K_0 K_1 + K_0^3) + K_1^2 (x^2 + y^2) \right] \quad (5)$$

$$y' = p_y - p_y p_\sigma \quad (6)$$

$$p_y' = y K_1 + K_2 x y$$

$$- \Gamma p_y \left[ K_0^2 (1 + 2p_\sigma) + x(2K_0 K_1 + K_0^3) + K_1^2 (x^2 + y^2) \right] \quad (7)$$

$$\sigma' = -K_0 x - \frac{p_x^2}{2} - \frac{p_y^2}{2} \quad (8)$$

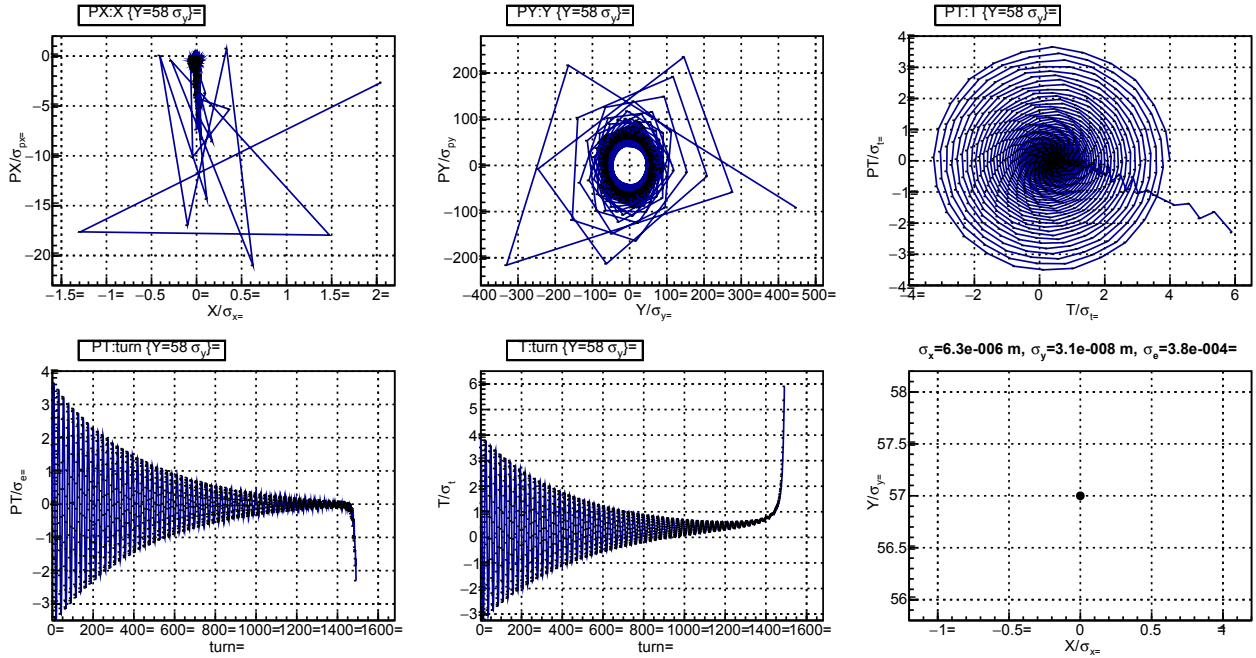


Figure 5: Phase and time trajectories of the first unstable particle with initial conditions  $\{x = 0, y = 58\sigma_y, p_x = 0, p_y = 0, \sigma = 0, p_\sigma = 0\}$ .

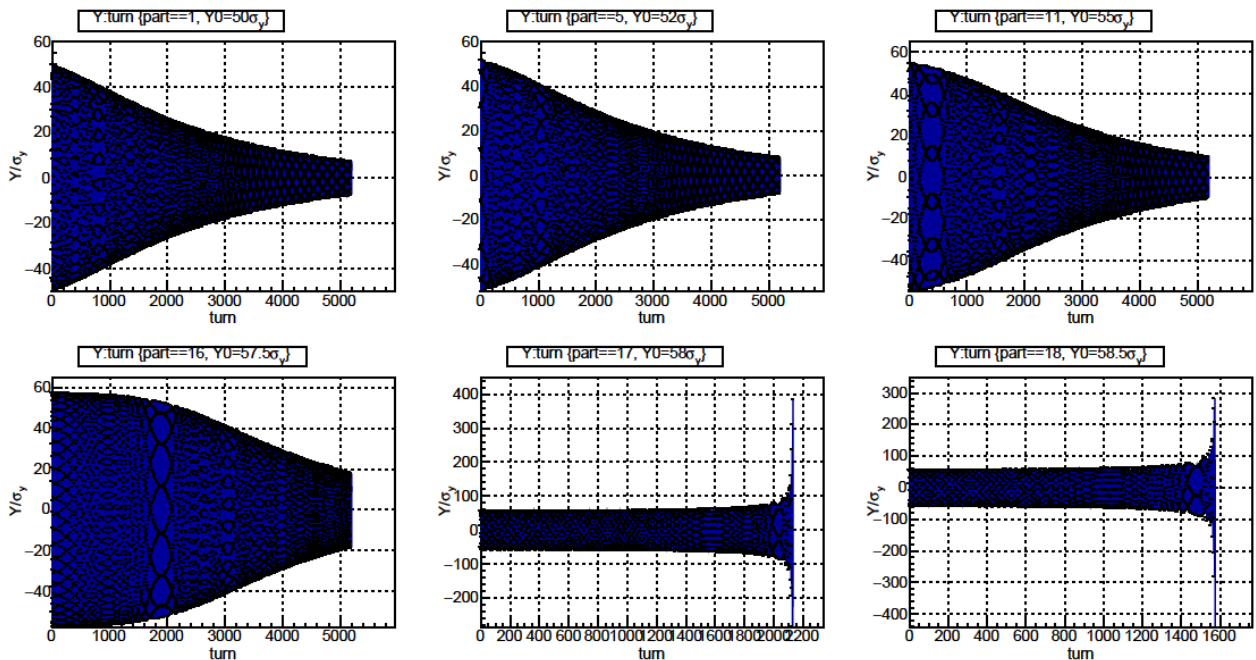


Figure 6: Time evolution of vertical oscillations for particles with initial vertical coordinate  $y = \{50; 52; 55; 57.5; 58; 58.5\} \times \sigma_y$ , horizontal coordinates are zero, longitudinal are adjusted for synchronous point.

Content from this work may be used under the terms of the CC BY 3.0 licence (© 2018). Any distribution of this work must maintain attribution to the author(s), title of the work, publisher, and DOI.

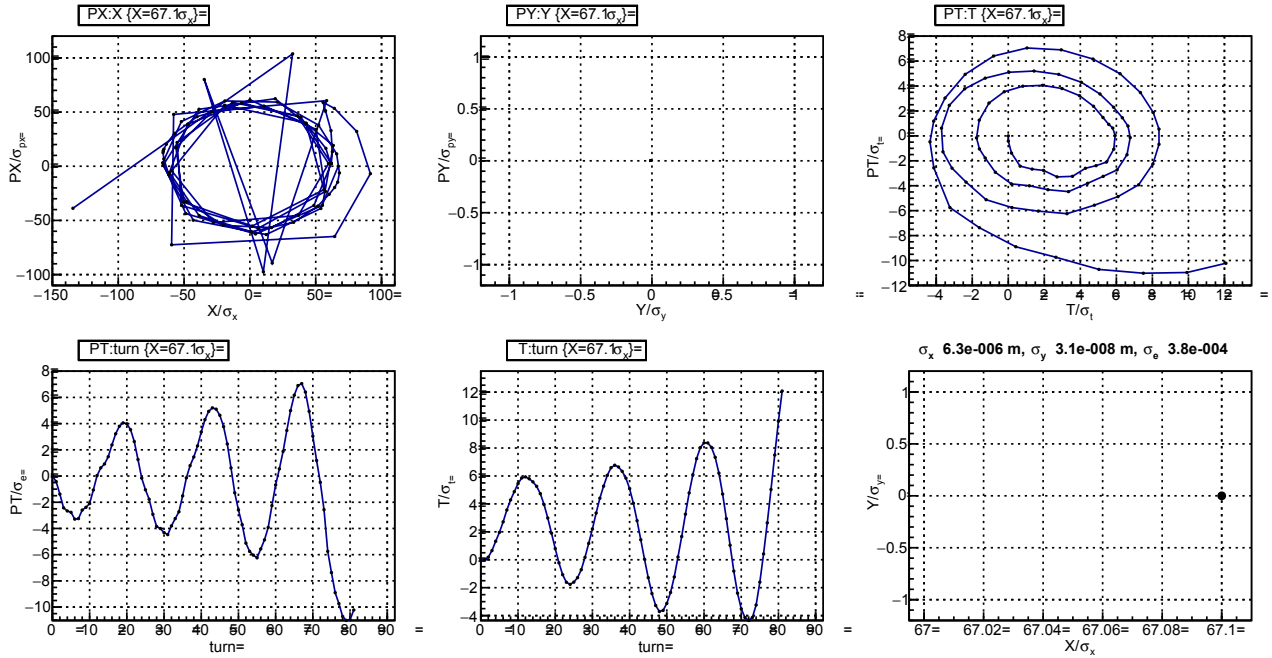


Figure 7: Phase and time trajectories of the first unstable particle with initial conditions  $\{x = 67.1\sigma_x, y = 0, p_x = 0, p_y = 0, \sigma = 0, p_\sigma = 0\}$ .

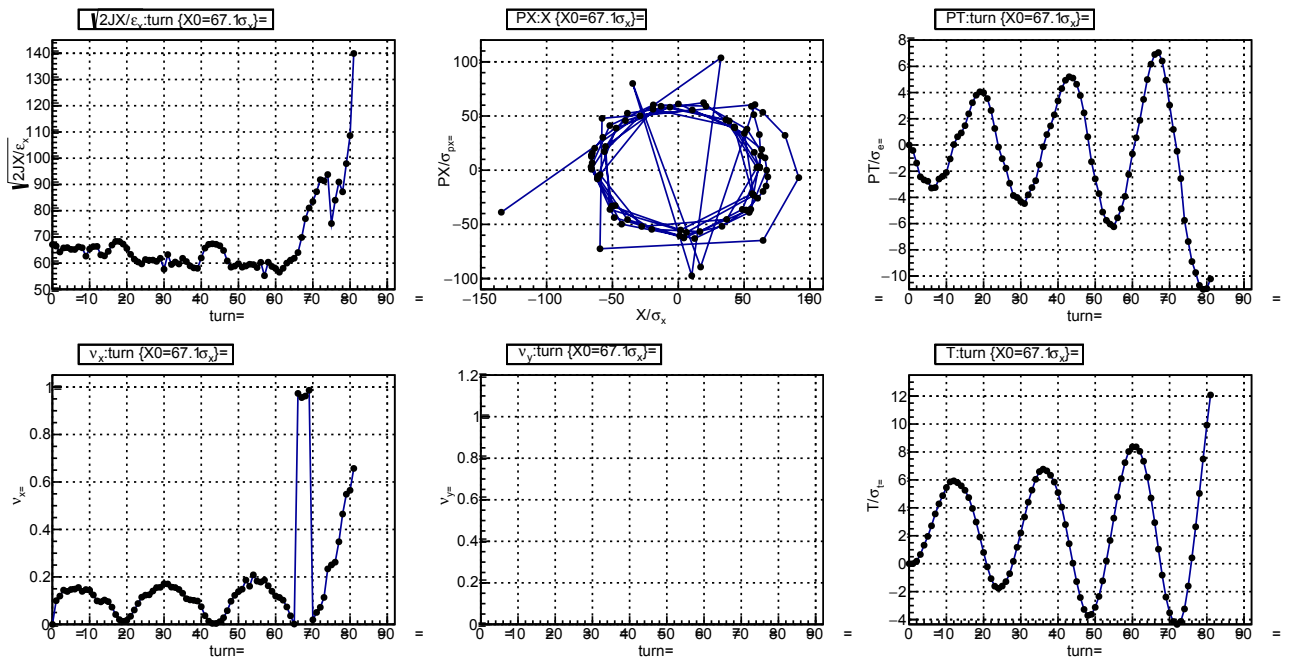


Figure 8: Square root of action and phase advance of the first unstable particle with initial conditions  $\{x = 67.1\sigma_x, y = 0, p_x = 0, p_y = 0, \sigma = 0, p_\sigma = 0\}$ .

$$p'_\sigma = \left( -\frac{eV_0}{p_0c} \right) \left( \sin \phi_s + \frac{2\pi\sigma}{\lambda_{RF}} \cos \phi_s \right) \delta(s - s_0) - \Gamma \left[ K_0^2(1 + 2p_\sigma) + x(2K_0K_1 + K_0^3) + K_1^2(x^2 + y^2) \right], \quad (9)$$

where  $\Gamma = \frac{C_\gamma}{2\pi} \frac{E_0^4}{p_0c}$ , and we expanded RF related  $\cos(\dots)$  to first order of  $\sigma$ .

## SOLUTION OF LONGITUDINAL EQUATIONS OF MOTION

At first, we will solve longitudinal equations of motion Eqs. (8) and (9) considering motion in the vertical plane and neglecting motion in the horizontal plane. Due to the fact that longitudinal motion is much slower than transverse (synchrotron oscillation frequency is lower than betatron), we consider vertical oscillation amplitude independent of time and solve decoupled equations. Splitting horizontal motion into betatron part and dispersion part  $x = x_\beta + \eta p_\sigma$ ,  $p_x = p_{x\beta} + \xi p_\sigma$ , neglecting betatron motion  $x_\beta = 0$ ,  $p_{x\beta} = 0$  yields equations

$$\sigma' = -K_0\eta p_\sigma - \xi^2 \frac{p_\sigma^2}{2} - \frac{p_z^2}{2} \quad (10)$$

$$p'_\sigma = \left( -\frac{eV_0}{p_0c} \right) \left( \sin \phi_s + \frac{2\pi\sigma}{\lambda_{RF}} \cos \phi_s \right) \delta(s - s_0) - \Gamma \left[ K_0^2 + p_\sigma(2K_0^2 + 2K_0K_1\eta + K_0^3\eta) + K_1^2(\eta^2 p_\sigma^2 + y^2) \right]. \quad (11)$$

Averaging of the obtained equations over the revolution period (as usually done for synchrotron motion) introduces familiar quantities: momentum compaction

$$\alpha = \langle K_0\eta \rangle = \frac{1}{\Pi} \oint K_0\eta ds, \quad (12)$$

the relative energy loss from dipoles per turn

$$\frac{1}{\Pi} \frac{U_0}{p_0c} = \Gamma \langle K_0^2 \rangle, \quad (13)$$

wave vector of synchrotron oscillations

$$k_s^2 = \frac{\alpha}{\Pi} \left( -\frac{eV_0}{p_0c} \right) \sum \frac{\pi}{\lambda_{RF}} \cos \phi_s = \left( \frac{\nu_s}{R} \right)^2, \quad (14)$$

longitudinal damping decrement

$$2\alpha_\sigma [m^{-1}] = \Gamma \langle (2K_0^2 + 2K_0K_1\eta + K_0^3\eta) \rangle = \frac{U_0}{\Pi p_0c} \left( 2 + \frac{\oint \sum K_0K_1\eta + K_0^3\eta ds}{\oint \sum K_0^2 ds} \right) = \frac{U_0}{\Pi p_0c} \left( 2 + \frac{I_4}{I_2} \right), \quad (15)$$

where  $\Pi = 2\pi R$  is the ring circumference,  $R$  is the average radius, angular brackets denote averaging over circumference  $\langle \dots \rangle = \oint \sum \dots ds / \Pi$ ,  $\nu_s$  is the synchrotron oscillations tune,

the RF field phase is chosen according to  $(-eV_0) \sin \phi_s = U_0$ ,  $I_4$  and  $I_2$  are the synchrotron integrals [13].

The factors  $\langle \xi^2 \rangle$  and  $\langle K_1^2 \eta^2 \rangle$  are small, and multiplication by  $p_\sigma^2$  makes them even smaller; therefore, we neglect them.

In order to deal with the terms  $y^2$  and  $p_y^2$ , we use the principal solution of the vertical motion equation [14]

$$y = A_y f_y + A_y^* f_y^* \quad (16)$$

$$p_y = A_y f_y' + A_y^* f_y^{*'},$$

where constant amplitude  $A_y$  depends on initial conditions,  $f_y$  is Floquet function with following properties

$$f_y = \sqrt{\beta_y} e^{i\psi_y}, \quad (17)$$

$$\psi_y(s) = \int_0^s \frac{d\tau}{\beta_y(\tau)}, \quad (18)$$

$$f_y f_y^{*'} - f_y' f_y^* = -2i, \quad (19)$$

$$f_y' = \frac{1}{\sqrt{\beta_y}} \left( \frac{\beta_y'}{2} + i \right) e^{i\psi_y}, \quad (20)$$

$$f_y' f_y^{*'} = \frac{1}{\beta_y} \left[ \left( \frac{\beta_y'}{2} \right)^2 + 1 \right] = \gamma_y, \quad (21)$$

$$f_y'^2 = \frac{1}{\beta_y} \left[ \left( \frac{\beta_y'}{2} \right)^2 - 1 + i\beta_y' \right] e^{i2\psi_y}, \quad (22)$$

where  $i$  is imaginary unit,  $\beta_y$  is beta function,  $\psi_y$  is betatron phase advance. Hence,

$$y^2 = (A_y f_y + A_y^* f_y^*)^2 = J_y \beta_y + A_y^2 f_y^2 + A_y^{*2} f_y^{*2}, \quad (23)$$

$$p_y^2 = (A_y f_y' + A_y^* f_y^{*'})^2 = J_y \gamma_y + A_y^2 f_y'^2 + A_y^{*2} f_y^{*2},$$

where action relates to amplitudes as  $J_y = 2A_y A_y^*$ , Twiss parameter gamma is  $\gamma_y = (1 + \alpha_y^2)/\beta_y$ ,  $\alpha_y = -\beta_y'/2$  and the subscript prime ' denotes  $d/ds$ .

In order to use Krylov-Bogolyubov averaging method we expand  $p_y^2$  and  $\Gamma K_1^2 y^2$  into Fourier series:

$$\Gamma K_1^2 y^2 = \Gamma K_1^2 \beta_y J_y + \Gamma A_y^2 e^{i2k_y s} \sum_{n=-\infty}^{\infty} F_{y,n} e^{in \frac{s}{R}} + \Gamma A_y^{*2} e^{-i2k_y s} \sum_{n=-\infty}^{\infty} F_{y,n}^* e^{-in \frac{s}{R}}, \quad (24)$$

$$p_y^2 = J_y \gamma_y + A_y^2 e^{i2k_y s} \sum_{n=-\infty}^{\infty} P_{y,n} e^{in \frac{s}{R}} + A_y^{*2} e^{-i2k_y s} \sum_{n=-\infty}^{\infty} P_{y,n}^* e^{-in \frac{s}{R}}, \quad (25)$$

where  $k_y = 2\pi\nu_y/\Pi = \nu_y/R$  is a wave vector of vertical betatron oscillations with tune  $\nu_y$ ,

$$F_{y,n} = \frac{1}{\Pi} \int_0^{\Pi} \sum K_1^2(s) f_y^2(s) e^{-i2k_y s - in \frac{s}{R}} ds = \frac{1}{\Pi} \int_0^{\Pi} \sum K_1^2(s) \beta_y(s) e^{i(2\psi_y(s) - 2\nu_y \frac{s}{R} - n \frac{s}{R})} ds, \quad (26)$$

$$P_{y,n} = \frac{1}{\Pi} \int_0^{2\pi} f_y'^2(s) e^{-i2k_y s - in \frac{s}{R}} ds$$

$$= \frac{1}{\Pi} \int_0^{2\pi} \frac{1}{\beta_y(s)} \left( \frac{\beta_y'(s)}{2} \right)^2 - 1 + i\beta_y'(s) \times \quad (27)$$

$$\times e^{i(2\psi_y(s) - 2\nu_y \frac{s}{R} - n \frac{s}{R})} ds.$$

Applying averaging method and keeping only slowly oscillating terms (Jowett omitted these terms in [15]) yields equations of motion

$$\sigma' = -\alpha p_\sigma - J_y \frac{\langle \gamma_y \rangle}{2}$$

$$- \frac{A_y^2}{2} P_{y,n} e^{i \frac{s}{R} (2\nu_y + n)} \quad (28)$$

$$- \frac{A_y^{*2}}{2} P_{y,n}^* e^{-i \frac{s}{R} (2\nu_y + n)},$$

$$p_\sigma' = \frac{k_s^2}{\alpha} \sigma - 2\alpha_\sigma p_\sigma - \Gamma \langle K_1^2 \beta_y \rangle J_y$$

$$- \Gamma A_y^2 F_{y,n} e^{i \frac{s}{R} (2\nu_y + n)} \quad (29)$$

$$- \Gamma A_y^{*2} F_{y,n}^* e^{-i \frac{s}{R} (2\nu_y + n)},$$

where  $n = -[2\nu_y]$  is the negative integer part of the double betatron tune and is the only slow oscillating harmonic.

### Synchronous Phase

Equating the right parts of the Eqs. (28) and (29) to zero and eliminating the oscillating terms results in synchronous longitudinal point

$$\sigma = -\frac{\alpha_\sigma}{k_s^2} \langle \gamma_y \rangle \sum_y + \frac{\alpha}{k_s^2} \Gamma \langle K_1^2 \beta_y \rangle J_y \quad (30)$$

$$p_\sigma = -\frac{1}{2\alpha} \langle \gamma_y \rangle J_y, \quad (31)$$

where the term with  $\Gamma$  corresponds to additional energy loss from radiation in quadrupoles, the other terms come from lengthening of particle trajectory. Jowett obtained similar equations in [6] and [16].

Particle with not adjusted initial conditions will develop synchrotron oscillations with respect to the new synchronous point. Using the longitudinal invariant

$$\sigma^2 + \frac{\alpha^2}{k_s^2} p_\sigma^2 = const \quad (32)$$

yields maximum energy deviation

$$p_{\sigma,max} = J_y \sqrt{-\frac{\alpha_\sigma \langle \gamma_y \rangle}{k_s \alpha} + \frac{\Gamma \langle K_1^2 \beta_y \rangle \sum_y^2}{k_s} + \frac{\langle \gamma_y \rangle^2}{4\alpha^2}} \quad (33)$$

### Solution without Oscillating Terms

Solution of Eqs. (28) and (29) without oscillating terms is known and consist of the constant term describing the shift of synchronous energy, and two terms describing damping

synchrotron oscillations (only for  $p_\sigma$ )

$$p_\sigma = -\frac{\langle \gamma_y \rangle}{2\alpha} \sum_y + B_1 e^{-\alpha_\sigma s} \cos \left( s \sqrt{k_s^2 - \alpha_\sigma^2} \right)$$

$$+ B_2 e^{-\alpha_\sigma s} \sin \left( s \sqrt{k_s^2 - \alpha_\sigma^2} \right) \sum \quad (34)$$

### Particular Solution

Introducing  $\mathfrak{x}_y = (2\nu_y + n)/R$  and transforming the system of first order differential Eqs. (28) and (29) into the the second order equation gives

$$p_\sigma'' + k_s^2 p_\sigma + 2\alpha_\sigma p_\sigma' =$$

$$- A_y^2 \left( \sum_s^2 P_{y,n} + i\Gamma \mathfrak{x}_y F_{y,n} \right) \sum i \mathfrak{x}_y s \quad (35)$$

$$- A_y^{*2} \left( \sum_s^2 P_{y,n}^* - i\Gamma \mathfrak{x}_y F_{y,n}^* \right) \sum -i \mathfrak{x}_y s.$$

Particular solution of Eq. (35) is

$$p_\sigma = -\frac{A_y^2 \left( \sum_s^2 P_{y,n} + i\Gamma \mathfrak{x}_y F_{y,n} \right)}{k_s^2 - \alpha_\sigma^2 + i2\mathfrak{x}_y \alpha_\sigma} e^{i \mathfrak{x}_y s}$$

$$- \frac{A_y^{*2} \left( \sum_s^2 P_{y,n}^* - i\Gamma \mathfrak{x}_y F_{y,n}^* \right)}{k_s^2 - \alpha_\sigma^2 - i2\mathfrak{x}_y \alpha_\sigma} e^{-i \mathfrak{x}_y s}.$$

Since

$$\mathfrak{x}_y \gg k_s \gg \alpha_\sigma, \quad (37)$$

$$\Gamma \mathfrak{x}_y |F_{y,n}| \gg \frac{k_s^2}{2\alpha} |P_{y,n}| \quad (38)$$

we can rewrite solution as

$$p_\sigma \approx i A_y^2 \frac{\Gamma F_{y,n}}{\mathfrak{x}_y} e^{i \mathfrak{x}_y s} - i A_y^{*2} \frac{\Gamma F_{y,n}^*}{\mathfrak{x}_y} e^{-i \mathfrak{x}_y s}. \quad (39)$$

Putting it in the form comfortable for the future use we have

$$p_\sigma = c_n A_y^2 e^{i \mathfrak{x}_y s} + c_n^* A_y^{*2} e^{-i \mathfrak{x}_y s}$$

$$= |c_n| J_y \cos(\mathfrak{x}_y s + \chi_0) \sum \quad (40)$$

where

$$c_n = -\frac{\left( \frac{k_s^2}{2\alpha} P_{y,n} + i\Gamma \mathfrak{x}_y F_{y,n} \right)}{k_s^2 - \alpha_\sigma^2 + i2\mathfrak{x}_y \alpha_\sigma} \approx i \frac{\Gamma F_{y,n}}{\mathfrak{x}_y} \quad (41)$$

and the phase  $\chi_0 = \arg(c_n A_y^2)$  depends on transverse initial conditions. The appearance of phase  $\chi_0$  is ambiguous, because in the averaging over the revolution period we lose all the information regarding particle initial transverse phase. Therefore, we will choose  $\chi_0$  in order to simplify further calculations.

## SOLUTION OF VERTICAL EQUATIONS OF MOTION

With the same assumptions as in the previous paragraph Eqs. (6) and (7) are

$$y' = p_y - p_y p_\sigma, \quad (42)$$

$$p_y' = K_1 y + K_2 \eta p_\sigma y - \Gamma p_y [K_0^2 + p_\sigma D + K_1^2 y^2], \quad (43)$$

where  $D = 2K_0^2 + 2K_0 K_1 \eta + K_0^3 \eta$  and for machines with separate functions magnets is negligible, we neglected the small term  $\Gamma p_y K_1^2 \eta^2 p_\sigma^2$ . We may apply Krylov-Bogolyubov averaging method directly to Eq. (42), Eq. (43), but it is more illustrative to apply it to  $y''$  equation. During derivation of  $y''$  equation we neglect the terms containing  $p_\sigma'$ , because it either oscillates with synchrotron tune or with double fractional part of betatron frequency, and after derivation will receive a small factor. The desired equation is

$$y'' - (K_1 - (K_1 - K_2 \eta) p_\sigma) y + \Gamma (K_0^2 + K_1^2 y^2) y' = 0. \quad (44)$$

This is an equation of parametric oscillator; the second term depends on  $p_\sigma$  which contains terms oscillating at fractional double betatron frequency Eq. (40). It is also a Van der Pol oscillator (nonlinear friction, the the third term). Jowett obtained Van der Pol equation for nonlinear wiggler (combined quadrupole and sextupole) in [16].

Substituting expression for  $p_\sigma$ , we neglect the constant shift and damped synchrotron oscillations Eq. (34), and keep only particular solution Eq. (40) oscillating on fractional part of double betatron frequency, i.e. we consider only parametric resonance. Substituting principal solution for  $y$  Eq. (16), averaging and keeping only slowly oscillating terms yields equation for amplitude evolution

$$\begin{aligned} (-2i)A_y' &= A_y \langle \Gamma K_0^2 (-\alpha_y + i) \rangle \\ &+ A_y^2 |c_n| \langle (K_1 - K_2 \eta) \beta_y e^{i(-2\psi_y + \alpha_{y,s} + \chi_0)} \rangle \\ &- 3A_y^2 A_y^* \langle \Gamma K_1^2 \beta_y \alpha_y \rangle \sum i A_y^2 A_y^* \langle \Gamma K_1^2 \beta_y \rangle. \end{aligned} \quad (45)$$

The terms  $\langle \Gamma K_1^2 \beta_y \alpha_y \rangle$  and  $\langle \Gamma K_1^2 \beta_y \rangle$  are small and we neglect them, obtaining

$$\begin{aligned} A_y' &= -\frac{1}{2} \langle \Gamma K_0^2 (1 + i\alpha_y) \rangle A_y \\ &+ \frac{i}{2} |c_n| \langle (K_1 - K_2 \eta) \beta_y e^{i(-2\psi_y + \alpha_{y,s} + \chi_0)} \rangle A_y^2 A_y^* \\ &= -B_1 A_y + iB_2 A_y^2 A_y^*. \end{aligned} \quad (46)$$

The real part of the obtained equation describes evolution of the  $A_y$  (e.g. damping), the imaginary part describes the change of the betatron tune. In order to solve Eq. (46) we introduce coefficients

$$B_1 = \frac{1}{2} \langle \Gamma K_0^2 (1 + i\alpha_y) \rangle \quad (47)$$

$$B_2 = \frac{1}{2} |c_n| \langle (K_1 - K_2 \eta) \beta_y e^{i(-2\psi_y + \alpha_{y,s} + \chi_0)} \rangle \quad (48)$$

where phase  $\chi_0$  appeared from Eq. (40) and is undefined. Multiplying Eq. (46) by  $A_y^*$  and adding a complex conjugate of the equation yields

$$(A_y A_y^*)' = -2Re(B_1) A_y A_y^* - 2Im(B_2) (A_y A_y^*)^2 \quad (49)$$

or

$$J_y' = -2Re(B_1) J_y \mp Im(B_2) J_y^2, \quad (50)$$

where  $J_y = 2A_y A_y^*$ ,  $Re()$  and  $Im()$  stand for real and imaginary parts. The first term describes damping of the action with vertical damping coefficient  $2Re(B_1) = \langle \Gamma K_0^2 \rangle$ , the second term if negative increases damping, if positive than counteracts damping. The sign of the second terms depends on the sign of the phase  $\chi_0$ , which appeared from solving averaged over revolution period longitudinal equations of motion Eqs. (35) and (40). Since longitudinal motion is slow than it can not depend on the phase of the transverse motion; whatever the phase was initially, it will change with time. Therefore, originally damping oscillations will change into rising oscillations (parametric resonance). Equation (50) solution is

$$J_y(s) = \frac{J_{y,0} e^{-2Re(B_1)s}}{1 \pm J_{y,0} \frac{Im(B_2)}{2Re(B_1)} (1 - e^{-2Re(B_1)s})}. \quad (51)$$

With appropriate sign before the second term, Eq. (50) permits existence of the boundary initial actions  $J_{y,lim}$ : lower initial actions will provide negative  $J_y'$  i.e. damping, larger will provide positive  $J_y'$  i.e. rising or unstable motion. This limiting action is the boarder of dynamic aperture and is

$$J_{y,lim} = \frac{2Re(B_1)}{\pm Im(B_2)}. \quad (52)$$

Existence of initial amplitudes with stable motion at parametric resonance is due to friction (radiation damping).

**Parametric resonance** In order to prove the choice of  $\chi_0$  we will solve Eq. (46) differently. Distinguishing modulus and argument of amplitude  $A_y = a_y e^{i\varphi_y}$ ,  $B_1 = |B_1| e^{i\varphi_1}$ ,  $B_2 = |B_2| e^{i\varphi_2 + i\chi_0}$  and substituting in Eq. (46) results in two equations

$$a_y' = -a_y |B_1| \cos(\varphi_1) - a_y^3 |B_2| \sin(-2\varphi_y + \varphi_2 + \chi_0) \quad (53)$$

$$\varphi_y' = -|B_1| \sin(\varphi_1) + a_y^2 |B_2| \cos(-2\varphi_y + \varphi_2 + \chi_0) \quad (54)$$

where  $|B_1| \sin(\varphi_1) = Im(B_1) = \frac{1}{2} \langle \Gamma K_0^2 \alpha_y \rangle \approx 0$  is small and describes the change of vertical betatron tune because of damping; this is equivalent to  $\varphi_1 = 0$ . The second term in Eq. (54) describes tune dependence on amplitude. Equations (53) and (54) have complex topology in  $\{a_y, \varphi_y\}$  space, which has two stable points  $\varphi_y = \varphi_2 + \chi_0 \pm \pi/4$  providing

$\varphi'_y = 0$ . At this points the modulus of amplitude is

$$a_y(s) = \frac{a_{y,0} e^{-|B_1|s}}{1 + a_{y,0}^2 \frac{|B_2|}{|B_1|} \sin(-2\varphi_y + \varphi_2 + \chi_0) (1 - e^{-|B_1|s})}$$

$$= \frac{a_{y,0} e^{-|B_1|s}}{1 \pm a_{y,0}^2 \frac{|B_2|}{|B_1|} (1 - e^{-|B_1|s})} . \quad (55)$$

The amplitude has two solutions: rising and damping. This is typical for parametric resonance and damping solution always changes into rising.

## LONGITUDINAL AND HORIZONTAL MOTION

Horizontal (Eqs. (4-5)) and longitudinal (Eqs. (8-9)) equations of motion with  $y = 0$  and  $p_y = 0$  are similar to longitudinal and vertical Eqs. (6-7) with  $x_\beta = 0$   $p_{x\beta} = 0$ . The unique for horizontal motion term  $-K_0 x_\beta$  in Eq. (8) will produce a synchro-betatron resonance at  $\nu_x \pm \nu_s = integer$ . This resonance plays an important role, but out of scope of our work. Table 3 shows that the shift of synchronous point and amplitude of synchrotron oscillations, if initial longitudinal coordinates are not adjusted to the new synchronous point, are significantly larger for horizontal oscillations than for vertical at the boundary of dynamic aperture. Observation of

Table 3: Synchronous point and amplitude of synchrotron oscillations for different transverse initial conditions

$\{X_0, Y_0\}$	$\{67\sigma_x, 0\}$	$\{0, 58\sigma_y\}$
$p_{\sigma,max}/\sigma_\delta$	4	0.26
$p_{\sigma,syn}/\sigma_\delta$	-2.5	-0.026
$\sigma_{syn}/\sigma_\delta$	3.05	0.29

phase advance per turn (bottom left) on Fig. 8 suggests that particle is lost when phase advance reaches an integer (turn 65) and it happens when  $p_\sigma = 7\sigma_\delta$ . Using the detuning coefficient and its chromaticity with initial conditions yields

Table 4: Tune shift contribution from detuning and detuning chromaticity

$\frac{\partial \nu_x}{\partial J_x}$	$-5 \times 10^4$
$\frac{\partial^2 \nu_x}{\partial J_x \partial \delta}$	$-6.8 \times 10^7$
$J_x$	$67^2 \varepsilon_x / 2$
$p_\sigma$	$7\sigma_\delta$
$\Delta \nu_x = \frac{\partial \nu_x}{\partial J_x} J_x$	-0.03
$\Delta \nu_x = \frac{\partial^2 \nu_x}{\partial J_x \partial \delta} J_x p_\sigma$	-0.11
$\nu_x(J_x = 0, p_\sigma = 0)$	0.14

## COMPARISON WITH TRACKING AND NUMERICAL ESTIMATIONS

For given vertical tune harmonic number is  $n = -534$ ,  $\varepsilon_y = 2.8 \times 10^{-5} \text{ m}^{-1}$ ,  $k_s = 2.6 \times 10^{-6} \text{ m}^{-1}$ . The harmonics Eqs. (26), (27) and (41) are

$$F_{y,n} = (-0.14, 3 \times 10^{-5}) \text{ m}^{-3} \quad F_{y,n} = 0.14 \text{ m}^{-3}$$

$$P_{y,n} = (-0.13, 0.0006) \text{ m}^{-1} \quad P_{y,n} = 0.13 \text{ m}^{-1}$$

$$c_n = (-42.11, -6474.19) \text{ m}^{-1} \quad |c_n| = 6474.33 \text{ m}^{-1} .$$

The numbers prove the inequality Eq. (38)

$$\Gamma \varepsilon_y F_{y,n} = 5.13 \times 10^{-6}$$

$$\frac{k_s^2}{2\alpha} P_{y,n} = 3.22 \times 10^{-8} .$$

Coefficients Eqs. (47) and (48) are

$$B_1 = (4.03 \times 10^{-9}, -2.76 \times 10^{-10}) \text{ m}^{-1}$$

$$|B_1| = 4.04 \times 10^{-9} \text{ m}^{-1}$$

$$B_2 = (10.35, 6.43) \text{ m}^{-2}$$

$$|B_2| = 12.18 \text{ m}^{-2} .$$

The border of dynamic aperture Eq. (52) is

$$R_y = \overline{2J_{y,lim}\beta_y} = 51.2\sigma_y , \quad (56)$$

which corresponds well to the tracking result  $R_y = 57\sigma_y$ .

Resemblance of longitudinal phase trajectories on Figs. 5 and 9 proves our approach in solving longitudinal Eqs. (28) and (29). Figure 9 presents numerical solution of the longitudinal Eqs. (28) and (29) with vertical action in the form Eq. (51) corresponding to initial condition  $y = 58\sigma_y$ .

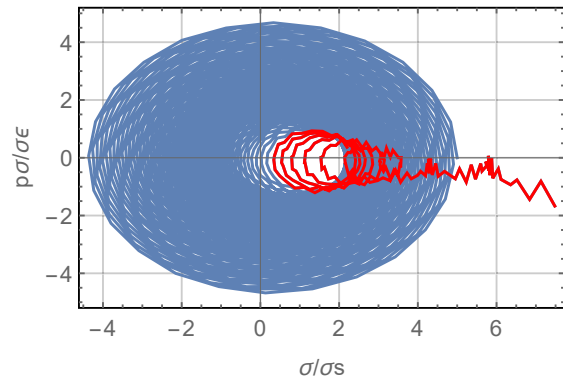


Figure 9: Longitudinal phase trajectories from numerical solution of Eqs. (28) and (29) with vertical action in the form Eq. (51) corresponding to initial condition  $y = 58\sigma_y$ . The last 200 turns are shown in red. Compare with top right plot of Figure 5.

Figure 10 and Fig. 11 compare results of tracking and calculations of longitudinal coordinate evolution (synchronous phase) when initial longitudinal conditions were adjusted

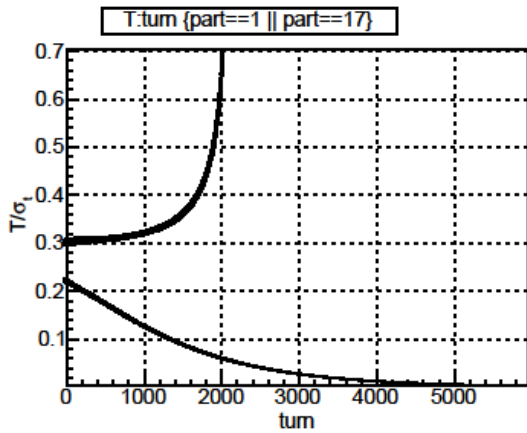


Figure 10: Evolution of longitudinal coordinate from tracking corresponding to initial conditions  $y = 50\sigma_y$  and  $y = 58\sigma_y$  and adjusted longitudinal initial conditions Eqs.(30) and (31).

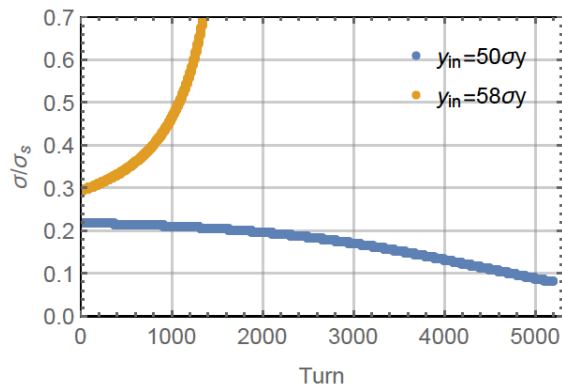


Figure 11: Evolution of longitudinal coordinate from calculations by Eqs. (30) and (31) corresponding to initial conditions  $y = 50\sigma_y$  and  $y = 58\sigma_y$ .

according to Eqs. (31) and (30) in order to eliminate synchrotron oscillations, for two particles with  $y = 50\sigma_y$  and  $y = 58\sigma_y$ .

Figure 12 and Fig. 13 show spectra of vertical and longitudinal motion, proving existence of fractional part of double betatron frequency in longitudinal motion. The double frequency harmonic amplitude according to Eq. (40) is  $p_\sigma = 3.6 \times 10^{-2}\sigma_\delta$ , which closely corresponds to the value on Fig. 13

Figure 14 and Fig. 15 compare vertical action evolution from tracking and calculation with Eq. (51). The boundary of stable motion is  $57.5\sigma_y$  from tracking and  $51\sigma_y$  from calculations by Eq. (52).

## CONCLUSION

In horizontal plane, additional energy loss due to radiation in quadrupoles, shifts synchronous point and develops large synchrotron oscillations. Horizontal betatron tune dependence on amplitude and chromaticity of this detuning shift the tune toward the integer resonance resulting in particle

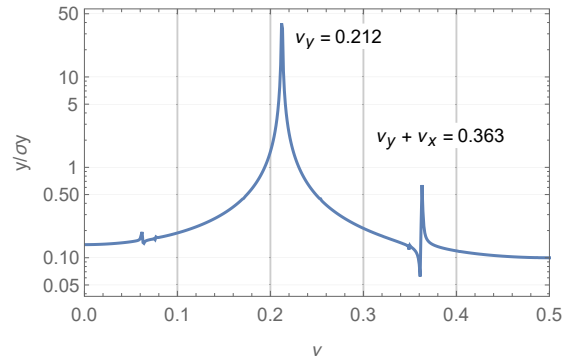


Figure 12: Spectrum of vertical motion tracking corresponding to initial condition  $y = 58\sigma_y$ , and adjusted longitudinal initial conditions Eqs. (30) and (31).

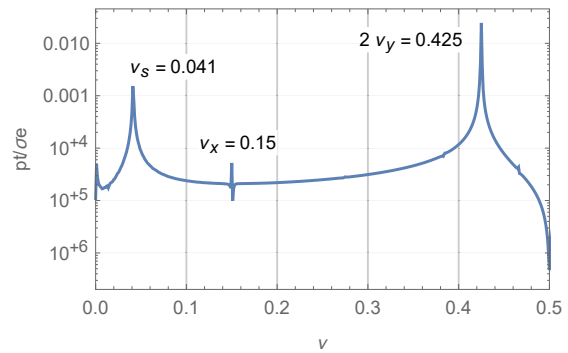


Figure 13: Spectrum of longitudinal motion tracking corresponding to initial condition  $y = 58\sigma_y$ , and adjusted longitudinal initial conditions Eqs. (30) and (31).

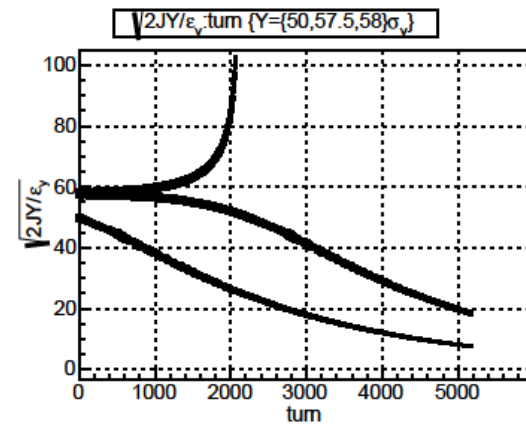


Figure 14: Evolution of normalized square root of vertical action from tracking corresponding to initial conditions  $y = 50\sigma_y$ ,  $y = 57.5\sigma_y$ ,  $y = 58\sigma_y$ , and adjusted longitudinal initial conditions in Eqs. (30) and (31).

loss. This is similar to Radiative Beta-Synchrotron Coupling (RBSC) proposed by Jowett [6].

Dynamic aperture reduction in the vertical plane with inclusion of synchrotron radiation in quadrupoles in FCC-ee is due to parametric resonance. Radiation from quadrupoles modulates the particle energy at the double betatron fre-

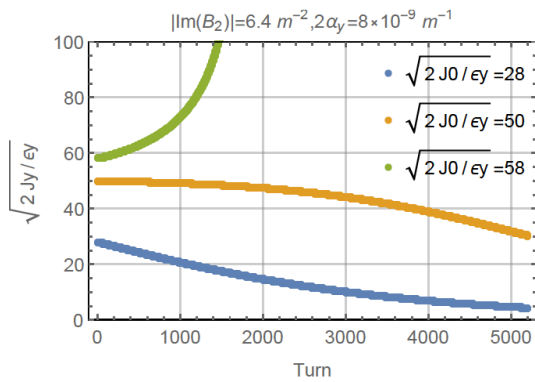


Figure 15: Evolution of normalized square root of vertical action from tracking corresponding to initial conditions  $y = 28\sigma_y$ ,  $y = 50\sigma_y$ ,  $y = 58\sigma_y$ .

quency; therefore, quadrupole focusing strength also varies at the doubled betatron frequency creating the resonant condition. However, due to friction, resonance develops only if oscillation amplitude is larger than a certain value. The remarkable property of this resonance is that it occurs at any betatron tune (not exactly at half-integer) and hence can be labeled as “self-inducing parametric resonance”. Our calculations give the border of dynamic aperture  $R_y = 51.2\sigma_y$ , which corresponds well to the tracking result  $R_y = 57\sigma_y$ .

## REFERENCES

- [1] FCC site: <http://cern.ch/fcc>
- [2] CEPC site: <http://cepc.ihep.ac.cn/>.
- [3] Augustin, J.E. and Dikansky, N. and Derbenev, Ya. and Rees, J. and Richter, Burton and others, “Limitations on performance of  $e^+e^-$  storage rings and linear colliding beam systems at high energy”, *eConf, C781015*, 1978, pp. 87-105.
- [4] Telnov, V. I., “Restriction on the energy and luminosity of  $e^+e^-$  storage rings due to beamstrahlung”, *Phys. Rev. Lett.*, 110(11), 2013, pp.114801-114806,
- [5] A. Bogomyagkov, E. Levichev, and D. Shatilov, “Beam-beam effects investigation and parameters optimization for a circular  $e^+e^-$  collider TLEP to study the Higgs boson”, *Phys. Rev. ST Accel. Beams* 17, (2014) 041004.
- [6] Jowett, J., “Dynamic aperture for LEP: Physics and calculations”, *Proceedings: LEP Performance Workshop*, 4th, Chamonix, France, Jan, 17-21, 1994, pp. 47-71.
- [7] Barbarin, F. and Iselin, F. C. and Jowett, J. M., “Particle dynamics in LEP at very high-energy”, *4th European Particle Accelerator Conference (EPAC 94) London*, England, June 27-July 1, 1994, pp. 193-195.
- [8] Jowett, John M., “Beam dynamics at LEP”, *CERN-SL-98-029-AP*, 1998., pp. 15-38.
- [9] SAD site: <http://acc-physics.kek.jp/SAD/index.html>
- [10] Oide, K. and others, “Design of beam optics for the Future Circular Collider  $e^+e^-$ -collider rings”, *Phys. Rev. Accel. Beams*, 19(11):111005, 2016 [Addendum: *Phys. Rev. Accel. Beams* 20, no.4, 049901(2017)].
- [11] MADX site: <http://madx.web.cern.ch/madx/>.
- [12] S. Glukhov and others, “6D Tracking with Compute Unified Device Architecture (CUDA) technology”, WEP34, *Proceedings of ICAP2015*, Shanghai, China, 2015, pp. 115-117.
- [13] Helm, Richard H. and Lee, Martin J. and Morton, P. L. and Sands, M., “Evaluation of synchrotron radiation integrals”, *Proceedings, 1973 Particle Accelerator Conference*, Accelerator Engineering and Technology: San Francisco, California, March 5-7, 1973, *IEEE Trans. Nucl. Sci.*, 20, 1973, pp. 900-901.
- [14] Courant, E. D. and Snyder, H. S., “Theory of the alternating gradient synchrotron”, *Annals Phys.*, 3, 1958, pp. 1-48 [Annals Phys.281,360(2000)].
- [15] Jowett, John M., “Introductory statistical mechanics for electron storage rings”, *AIP Conf. Proc.*, 153, 1987, pp. 864-970.
- [16] Jowett, John M., “Electron dynamics with radiation and non-linear wigglers”, *CERN Accel.School* 1985:0570, 1986.